Electrical Power and Energy Systems 118 (2020) 105743

Contents lists available at ScienceDirect

Electrical Power and Energy Systems

journal homepage: www.elsevier.com/locate/ijepes

Thermal performance of transformers filled with environmentally friendly oils under various loading conditions

Mohamed M.M. Salama[a], Diaa-Eldin A. Mansour[b,*], Muhammad Daghrah[c], Samir Mohamed Abdelkasoud[a], Ahmed A. Abbas[a]

[a] *Department of Electrical Power and Machines Engineering, Faculty of Engineering at Shoubra, Benha University, Cairo, Egypt*
[b] *Department of Electrical Power and Machines Engineering, Faculty of Engineering, Tanta University, Tanta, Egypt*
[c] *M&I Materials Ltd, Manchester, UK*

ARTICLE INFO

Keywords:
Environmentally friendly oils
Hot spot temperature
Top oil temperature
Thermal performance
Transformer aging

ABSTRACT

The transformer thermal performance is a crucial issue that should be considered in the design stage. Recently, natural and synthetic ester oils have been proposed as environmentally friendly oils to substitute conventional mineral oil. This paper aims to evaluate the transformer thermal performance when using these environmentally friendly oils under different loading power factors. Three commercial types of environmentally friendly oils are considered, Midel 1204 and Midel 1215 as natural esters and Midel 7131 as a synthetic ester. Thermal-related properties of these esters are experimentally evaluated. These results include viscosity, thermal conductivity, specific heat capacity, and density. The experimental data is used to find a best representative formula for the thermo physical properties of these oils as a function of operating temperature by using least square regression method. A model 3D CFD COMSOL model is built including heat transfer model and laminar flow model to calculate the rated top oil temperature (TOT) and the rated winding hottest spot temperature (HST) for these environmentally friendly oils and for mineral oil. The rated output TOT and HST from COMSOL are used as inputs for a developed MATLAB model through which TOT and HST all day long can be obtained. Using these models, the TOT and HST for transformers filled with mineral oil and environmentally friendly oils are obtained. Also, the transformer aging and loss of life are assessed with these oils for the different scenarios of the loading power factor (PF). Finally, the annual energy losses of the transformer, their cost, and their impact on greenhouses gases emissions and corresponding environmental cost are evaluated as key issues for making proper decisions toward using environmentally friendly oils. It was found that using environmentally friendly oils reduces significantly the transformer aging compared to using mineral oil for different loading PFs.

1. Introduction

The basic objectives of the transformers are to step-up the voltage at the generating stations and step-down the voltage at electric network utilization to mitigate the losses and voltage drop [1]. The loadability of the transformer can be checked by the thermal limit of the transformer. The reference winding hottest spot temperature (HST) of the transformer represents the transformer thermal limit. Hence, the transformer thermal performance plays a vital role in the load flow analysis. If HST exceeds the reference value, the real life of the transformer will be reduced. An accurate transformer thermal model should be used to monitor and simulate the winding HST. The main reason of the internal heat generation is the transformer's losses. They include the winding ohmic losses, the winding eddy current losses, no-load losses, and the other stray losses in the structural parts and the wall tanks. If the dissipation of the transformer internal heat generation is increased, the transformer capability will be increased [2].

The transformer oil has a crucial role in the heat dissipation of the internal heat generation to the ambient. The oil thermal performance is affected by the oil thermal properties such as viscosity, thermal conductivity, specific heat, density, and volumetric thermal expansion coefficient [3]. Since 1892, mineral oil which is extracted from the petroleum is used for transformers applications. The demerits of mineral oil are poor biodegradability (30% biodegradability level), low flash point, depleted, not environment-friendly and serious problems are found if a spillage is occurred. Hence, transformer manufacturers are recently using environmentally friendly oils such as natural esters and synthetic ester. The esters have high biodegradability level

* Corresponding author.
E-mail address: mansour@f-eng.tanta.edu.eg (D. A. Mansour).

https://doi.org/10.1016/j.ijepes.2019.105743
Received 20 August 2019; Received in revised form 20 October 2019; Accepted 25 November 2019

(> 95%), offer higher flash point (> 300 °C) and fire point (> 300 °C), have higher acidity and absorb more moisture compared to the mineral oil [4–6]. The different types of the natural ester oils are for example rapeseed, soya, sunflower, palm, etc.

The load power factor (PF) is a power quality issue. If it has a low value, it can cause degradation of equipment. The main demerit of a low PF is increasing the current with a subsequent increase in the voltage drop and the losses. If the load PF is improved, this will increase the system capacity [7–9]. In this paper, the thermal performance, aging and energy losses cost of transformers filled with environmentally friendly oils are investigated considering the impacts of ambient temperature and load PF. Also, the greenhouses gases (GHG) emissions cost due to the transformer energy losses that will lead to additional combustion of fossil fuels into the generation plants are considered. The top oil temperature (TOT) and HST are simulated for the mineral and the environmentally friendly oils considering the different loading PF values. The loading current is considered all day long for annual average load PF of 0.85, 0.9, and 0.95 lagging. A numerical analysis is used by computational fluid dynamics (CFD) software (COMSOL) to find the rated TOT and HST for the transformer filled with the alternative oils. A 630 kVA, ONAN cooling type, oil-filled transformer is considered. In spite of many researchers in [10–18] investigated thermal and dielectric properties of environmentally friendly oils, none of these studies evaluated to what extent the esters can affect the transformer aging, the transformer loadability (by evaluating HST all day long), the cost of the transformer total energy losses, the GHG emissions, the environmental cost, and the enhancement cost of the loading power factor. Evaluating these issues is the main contribution of this paper that can provide guidelines for the power system operators to make the proper plan and design towards using these alternative oils.

2. Characterization of load power factor

The transformer loading has been considered at each instant all day long with annual average load PF of 0.85, 0.9 and 0.95 lagging as shown in Fig. 1. The improved load PF decreases the transformer heating and increases the transformer capacity to feed additional load. For determining to what extent the transformer capacity will be increased, the ambient temperature and the transformer thermal parameters should be considered to monitor HST. For example, the load PF may be improved from 0.85 to 0.95 lagging but the ambient temperature for the loading of 0.95 lagging PF is higher than that for 0.85 lagging PF. In this case, the transformer capacity of 0.95 lagging PF may not be increased due to the heat dissipation to the ambient is reduced than that of 0.85 lagging PF. In this paper, the ambient temperature is maintained the same to consider the impact of changing PF on the thermal performance considering alternative oils having different thermal properties.

3. Experimental results of environmentally friendly oils

The oil thermal-related properties such as viscosity, thermal conductivity, specific heat capacity, density, and volumetric thermal

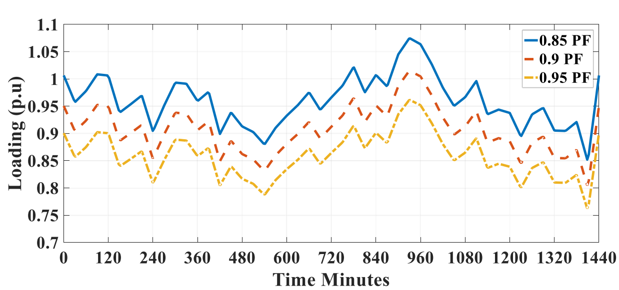

Fig. 1. The daily pu loading for the three dedicated load PF.

expansion coefficient have great impact on the transformer thermal performance. These properties are dependent on the operating temperature of the oil. To calculate the rated TOT and HST, the models of the thermal properties must be considered into COMSOL. Also, they are needed under wide range of the operating temperatures to calculate TOT and HST all day long into MATLAB. In this paper, experiments were carried out by Midel to measure the kinematic viscosity, density, thermal conductivity, and specific heat capacity for synthetic ester (Midel 7131), rapeseed (Midel 1204), and soya (Midel 1215) with temperature range from −10 °C to 100 °C. The experimental data is used to find a best representative formula for the natural ester and synthetic ester oils thermo physical properties as a function of operating temperature by using least square regression method. The goodness fit of the measurements can be evaluated by a correlation coefficient which is called R-square. It can be formulated as the following: [19]

$$\mathrm{R-square} = \frac{\mathrm{SSR}}{\mathrm{SST}} = 1 - \frac{\mathrm{SSE}}{\mathrm{SST}} \tag{1}$$

where:

SST: total sum of squares
SSR: sum of squares of the regression
SSE: sum of squares because of error

3.1. Dynamic viscosity

The measured values of the kinematic viscosity are multiplied by the density to obtain the dynamic viscosity which is modelled as a temperature dependence numerical model as in Eq. (2). The standard test method used for measuring the kinematic viscosity is ISO 3104. Table 1 shows the actual test results of the kinematic viscosity which is multiplied by the density at different temperatures for the different types of esters. Table 2 shows the fit parameters of the dynamic viscosity model for each type of esters. In [20], the dynamic viscosity of the mineral oil is modelled as in Eq. (3). When the oil temperature is increased the viscosity will be decreased as shown in Fig. 2.

$$\mu = \mathrm{a}e^{\mathrm{b}\theta_{\mathrm{oil}}} + \mathrm{c}e^{\mathrm{d}\theta_{\mathrm{oil}}} \tag{2}$$

$$\mu = 7.863 \times 10^{-5} e^{\frac{632}{\theta_{\mathrm{oil}}+97.15}} \tag{3}$$

where:

μ: dynamic viscosity ($kg\ \ m^{-1}s^{-1}$)
θ_{oil}: top oil temperature °C
a, *b*, *c*, *d*: exponential fit parameters of dynamic viscosity

3.2. Thermal conductivity

The standard test method used for measuring the thermal conductivity is ASTM D7896. Table 3 shows the actual test results of the

Table 1
Actual test results of dynamic viscosity for ester oils (kgm^{-1}s^{-1}).

Temperature (°C)	Midel 7131	Midel 1204	Midel 1215
−10	0.5661084	0.421162	0.317791
0	0.2288992	0.21413	0.193752
10	0.1179871	0.1221	0.090113
20	0.07229466	0.07803	0.061774
30	0.0413058	0.051984	0.042136
40	0.02812235	0.033485	0.029088
50	0.018447	0.025144	0.021648
60	0.01286156	0.018732	0.016647
70	0.009316	0.01416	0.0128016
80	0.00711788	0.010548	0.010143
90	0.00568664	0.0086328	0.0081375
100	0.004823	0.0071878	0.0065968

Table 2
Dynamic viscosity exponential fit parameters for ester oils.

Ester Sample	Midel 7131	Midel 1204	Midel 1215
a	0.0815	0.103	0.1599
b	−0.1439	−0.09655	−0.06236
c	0.1478	0.1117	0.02055
d	−0.04087	−0.02984	−0.009762
R-square	0.9999	0.9999	0.9959

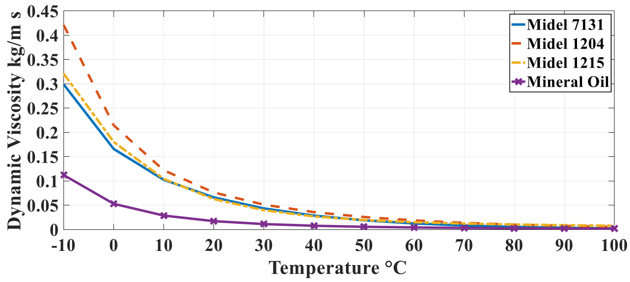

Fig. 2. Temperature dependence of the dynamic viscosity measurements for the three esters and the mineral oil.

Table 3
Actual test results of thermal conductivity for ester oils ($Wm^{-1}K^{-1}$).

Temperature (°C)	Midel 7131	Midel 1204	Midel 1215
−10	0.149	0.179	0.167
0	0.148	0.179	0.167
10	0.148	0.178	0.167
20	0.147	0.177	0.166
30	0.147	0.176	0.166
40	0.146	0.175	0.165
50	0.145	0.173	0.164
60	0.144	0.172	0.164
70	0.142	0.17	0.163
80	0.141	0.167	0.162
90	0.139	0.165	0.161
100	0.138	0.162	0.16

Table 4
Thermal conductivity polynomial fit parameters for ester oils.

Ester Sample	Midel 7131	Midel 1204	Midel 1215
e	3.478×10^{-22}	-2.979×10^{-9}	1.554×10^{-9}
f	-7.193×10^{-7}	-7.742×10^{-7}	-6.194×10^{-7}
g	-3.526×10^{-5}	-5.939×10^{-5}	-2.273×10^{-5}
h	0.1484	0.1787	0.167
R-square	0.9927	0.9979	0.9906

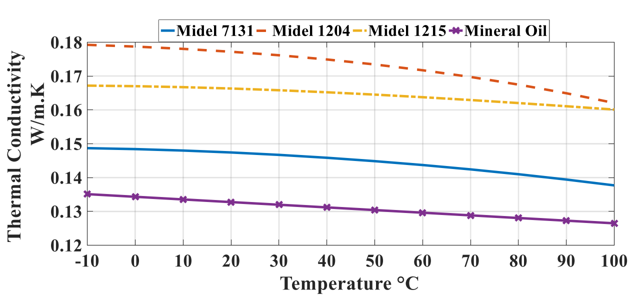

Fig. 3. Thermal conductivity measurements versus temperature for the three esters and the mineral oil.

Table 5
Actual test results of specific heat for ester oils (J/kg.° C).

Temperature (°C)	Midel 7131	Midel 1204	Midel 1215
−10	1851	1798	1920
0	1860	1816	1934
10	1880	1833	1946
20	1902	1849	1970
30	1919	1864	1986
40	1945	1879	2011
50	1969	1895	2038
60	1995	1911	2066
70	2020	1929	2096
80	2052	1947	2122
90	2076	1968	2155
100	2105	1990	2186

thermal conductivity at different temperatures for the different types of esters. The measured thermal conductivity of the Midel 7131, Midel 1204, and Midel 1215 oils is fitted as a third-degree polynomial equation against the temperature as in Eq. (4). The thermal conductivity polynomial fit parameters of the thermal conductivity equation for each ester are shown in Table 4. In [20], the thermal conductivity of the mineral oil is modeled as in Eq. (5). Fig. 3 shows the thermal conductivity versus temperature for the three types of esters and mineral oil.

$$k = e\theta_{oil}^3 + f\theta_{oil}^2 + g\theta_{oil} + h \quad (4)$$

$$k = -7.837 \times 10^{-5} \times (\theta_{oil}+273.15) + 0.1557 \quad (5)$$

where:

k: thermal conductivity ($W \ m^{-1}K^{-1}$)
e, f, g, h: polynomial fit parameters of thermal conductivity

3.3. Specific heat

The standard test method used for measuring the specific heat is ASTM E1269. Table 5 shows the actual test results of the specific heat at different temperatures for the different types of esters. The measured values of the specific heat for each ester are represented as a third-degree polynomial equation as in Eq. (6) and the polynomial fit parameters are shown in Table 6. In [20], the specific heat of the mineral oil is modelled as in Eq. (7). The specific heat of the oil is temperature dependent as shown in Fig. 4.

$$C_p = i\theta_{oil}^3 + j\theta_{oil}^2 + k\theta_{oil} + l \quad (6)$$

$$C_p = 3.95 \times (\theta_{oil} + 273.15) + 560.2 \quad (7)$$

where:

C_p: specific heat ($J/kg.^{\circ}$ C)

Table 6
Specific heat capacity polynomial fit parameters for ester oils.

Ester Sample	Midel 7131	Midel 1204	Midel 1215
i	-5.698×10^{-5}	6.229×10^{-5}	-5.698×10^{-5}
j	0.01454	−0.006089	0.01713
k	1.531	1.728	1.389
l	1863	1816	1933
R-square	0.9996	1	0.9996

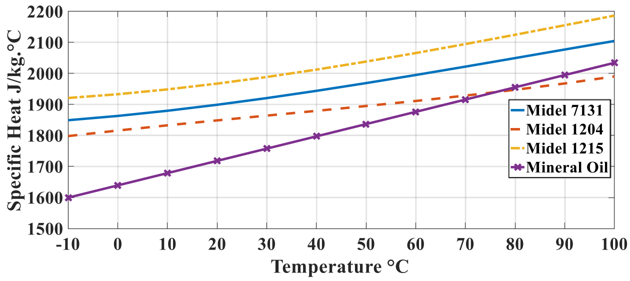

Fig. 4. Experimental measurements of the specific heat capacity versus the temperature for the three esters and the mineral oil.

Table 7
Actual test results of oil density for ester oils (kgm^{-3}).

Temperature (°C)	Midel 7131	Midel 1204	Midel 1215
−10	989.7	938	943
0	982.4	931	936
10	975.1	925	929
20	967.8	918	922
30	960.6	912	916
40	953.3	905	909
50	946	898	902
60	938.8	892	895
70	931.6	885	889
80	924.4	879	882
90	917.2	872	875
100	910	866	868

Table 8
Ester density polynomial fit parameters for ester oils.

Ester Sample	Midel 7131	Midel 1204	Midel 1215
o	−0.7245	−0.6563	−0.6776
p	982.3	931.3	936
R-square	1	0.9998	0.9999

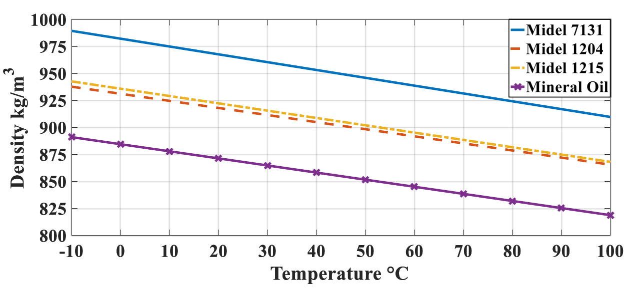

Fig. 5. Experimental measurements of oil density versus temperature for the three esters and the mineral oil.

i, j, k, l: polynomial fit parameters of specific heat

3.4. Density

The standard test method used for measuring the density is ISO 3675. Table 7 shows the actual test results of the density at different temperatures for the different types of esters. The experimental data of the three esters is expressed as a first-degree polynomial equation which is a function of temperature as in Eq. (8) and the polynomial fit parameters are shown in Table 8. In [20], the mineral oil density is modelled as in Eq. (9). The temperature dependence of the oil density is shown in Fig. 5.

$$\rho = o\theta_{oil} + p \quad (8)$$

$$\rho = -0.6568 \times (\theta_{oil} + 273.15) + 1064 \quad (9)$$

where:

ρ: oil density ($kg \ m^{-3}$)
o, p: polynomial fit parameters of density

4. Numerical analysis

A 3D CFD COMSOL model is used to calculate the rated TOT and the rated HST for the mineral oil, Midel 7131, Midel 1204, and Midel 1215. COMSOL is a powerful tool which can be used in a steady state case study or in a transient case study. The heat transfer model and the laminar flow model are two models which can be coupled internally into COMSOL to simulate the rated HST at steady state condition. As the simulation time of COMSOL is around twenty minutes for this steady state case study, the output rated TOT and HST from COMSOL are used as input for MATLAB. Transformer thermal model of Susa [10,11] is modelled by MATLAB to simulate TOT and HST all day long with less than 3 s simulation time. In general, the heat transfer model and the laminar flow model of the COMSOL are validated for the different sizes of the transformer applications as in [14,17,18]. Also Susa's model is validated for different sizes of the transformers as in [10,11]. The calculations for the mineral oil case are matched with the manufacturing data. As per the manufacturer of the mineral oil-filled transformer, the rated TOT is 79.7 °C and the rated HST is 96.2 °C. But, the simulated rated TOT is 80.6 °C and the simulated rated HST is 97 °C. The heat transfer into the solid and the fluid is coupled with the laminar flow internally built into COMSOL. A 630 kVA transformer is the dedicated one for this paper. The low voltage (LV) winding is made of copper foil with star connection and the high voltage (HV) winding is made of copper round wire with delta connection. It is a core type with two large individual cores and two small individual cores. As per the manufacturer, the transformer parameters in Table 9 are used to build the model into COMSOL. The mesh is considered a physics-controlled mesh with extra fine element size. The thermal parameters of the mineral oil and alternative oils are defined for this model as in Eqs. (2)–(9). After calculating the rated TOT and HST under rated ambient temperature by using COMSOL at steady state case study, the calculated rated TOT and HST is used as input for Susa's model. In Section 5, Susa model is modelled into MATLAB programming language to simulate TOT and HST variations all day long.

4.1. Heat transfer

For establishing the model into COMSOL, the losses into the windings, the core, and the wall tanks are introduced as heat sources for this model. The heat sources are considered as an overall heat transfer rate. The rated winding losses of the dedicated transformer are 9688 W, the rated other stray losses are 1350 W, and the no-load losses are 1195 W. The overall heat transfer rate for the one phase winding is 3229.3 W, for the small core is 280.27 W, for the large core is 317.23 W, for the wall

Table 9
Parameters of 630 kVA oil-filled transformer.

Cross-section area of LV winding	191.18 mm2
Width of LV conductor	242 mm
Thickness of LV conductor	0.79 mm
Number of turns of LV winding	15
Resistance of LV winding	0.00156 Ω
Diameter of HV conductor without insulation	1.8 mm
Number of turns of HV winding	1299
Resistance of HV winding	4.2 Ω
Tank length	1317 mm
Tank width	620 mm
Tank height	803 mm

tank is 1350 W. The governing Eqs. (10) and (11) are for heat transfer in solid and liquid respectively. The heat transferred to the ambient temperature by convective is shown in Eq. (12) [21,22].

$$\rho C_p u.\ \nabla\theta + \nabla.(-k\nabla\theta) = Q - \alpha\theta:\frac{dS}{dt} \quad (10)$$

$$\rho C_p u.\ \nabla\theta + \nabla.(-k\nabla\theta) = Q + \alpha\theta\left(\frac{\partial p}{\partial t} + u.\ \nabla p\right) + \tau:\ \nabla u \quad (11)$$

$$-n.\ q_r = \varepsilon\sigma({\theta^4}_{amb} - \theta^4) \quad (12)$$

where:

u: velocity vector (m/s)
θ: absolute temperature (°C)
θ_{amb}: ambient temperature profile (°C)
Q: heat sources (Wm^{-3})
α: coefficient of thermal expansion (K^{-1})
S: second Piola-Kirchhoff stress tensor (Pa)
$\frac{d}{dt}$: material derivative
p: pressure (Pa)
τ: viscous stress tensor (Pa)
n: refractive index of the media
σ: Stefan-Boltzmann constant) $Wm^{-2}K^{-4}$(
ε: surface emissivity
q_r: radiative heat flux

4.2. Laminar flow

The laminar flow is coupled with the heat transfer internally into COMSOL to study the impact of filling the transformer with alternatives to the mineral oil on the liquid flow and temperature. In [23], the winding inlet velocity for the mineral oil is (15 mm/s) and the pressure is considered zero at the output. In [24], the ester velocity is related to the mineral oil as shown in Eq. (13). In [21,22], the governing Eq. (14) is for the laminar flow.

$$\frac{{V^2}_{in,ester}}{{V^2}_{in,mineral}} = \frac{(\alpha/\nu * C_p * \rho)_{ester}}{(\alpha/\nu * C_p * \rho)_{mineral}} \quad (13)$$

$$\rho(u.\ \nabla)u = \nabla.\left[-\rho I + \mu(\nabla u + (\nabla u)^{\theta}) - \frac{2}{3}\mu(\nabla.\ u)I\right] + F \quad (14)$$

where:

$V_{in,ester}$: winding inlet velocity for ester case ($mm\ \ s^{-1}$)
$V_{in,ester}$: winding inlet velocity for mineral oil case ($mm\ \ s^{-1}$)
ν: Kinematic viscosity($mm^2\ \ s^{-1}$)
F: volume force vector ($N\ \ m^{-3}$)

5. Transformer thermal model

The transformer thermal model must be more rigorous for operation of the transformer close to the winding HST limit. This can minimize the secure margin and the unused capacity [25]. The heat transfer approach is applied by using the thermal-electrical analogy to figure the winding HST and TOT. The oil viscosity inconstancy effect on the oil temperature has been considered in this model. The winding HST and TOT variations are calculated with the changes of the ambient temperature and the loading with time constant. Susa's model is used for modelling the transformer thermal performance into MATLAB programming language by interconnecting two separate models. The first model is TOT model to simulate TOT changes with the ambient temperature and the loading with the oil time constant. TOT is used as input for the winding HST model which is the second model. HST model is used to simulate the winding HST changes with the loading and TOT variations with the winding time constant [11]. Hence, the alternatives of mineral oil will affect the oil temperature profile and subsequently the winding HST profile. The profile of ambient temperatures changes all day long is shown in Fig. 6. The thermal parameters of a 630 kVA oil-filled transformer with oil natural air natural cooling type are shown in Table 10. The cooling exponents vary with respect to the cooling type as shown in Table 11.

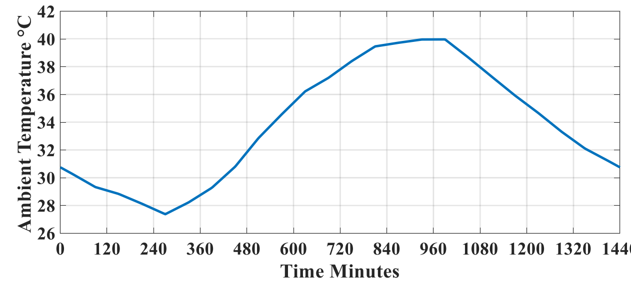

Fig. 6. The ambient temperature profile all day long.

Table 10
Thermal parameters of 630 kVA oil-filled transformer.

(I^2R) Rated losses of windings losses	9023 W
P_{EC-R}(Rated eddy current losses)	665 W
P_{OSl-R}(Other stray losses under rated conditions)	1350 W
No Load loss	1195 W
P.U eddy current losses at the hot spot location	0.72
Ratio of rated load losses to no load losses	9.24

Table 11
Thermal model exponents for cooling types [26]

Cooling types	n'	n"
No external cooling	0.25	0.25
With external cooling	2	0.5

5.1. Top oil temperature model

To calculate TOT for the mineral oil and the alternative oils, the thermal-related properties such as the thermal conductivity, viscosity, specific heat, density, and volumetric thermal expansion coefficient should be taken into account. Fig. 7 shows the structure of building TOT model into MATLAB [11]. The top oil temperature model can be calculated as follows [27]:

$$\frac{1 + R \times K^2}{1 + R} \times {\mu_{pu}}^{n''} \times \Delta\theta_{oil,rated} = {\mu_{pu}}^{n''} \times \tau_{oil,rated} \times \frac{d\theta_{oil}}{dt} + \frac{(\theta_{oil} - \theta_{amb})^{1+n''}}{\Delta\theta_{oil,rated}^{n''}} \quad (15)$$

$$\tau_{oil,rated} = C_{th-oil,rated}\frac{\Delta\theta_{oil,rated}}{q_{tot,rated}} \times 60 \quad (16)$$

where:

$\Delta\theta_{oil,rated}$: rated TOT rise over the ambient temperature (°C)
$\tau_{oil,rated}$: oil time constant under rated conditions (minutes)
K: the per unit loading based on the rated load
$q_{tot,rated}$: rated total losses of the transformer (watt)
R: transformer rated load losses attribution to no-load losses
μ_{pu}: oil viscosity as per-unit
$C_{th-oil,rated}$: oil thermal capacitance under rated conditions (joules /°C)
n'': cooling exponent for air moving fluid

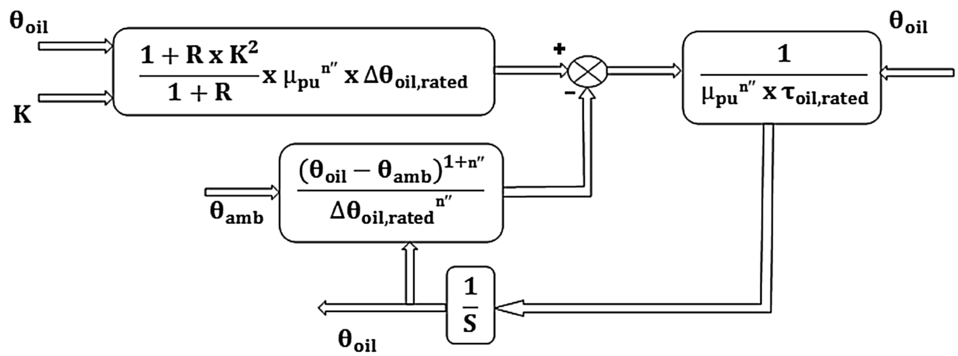

Fig. 7. Block diagram of the top oil temperature model.

The oil thermal capacitance of the transformer with external cooling can be expressed as follows [11]:

$$C_{th-oil} = Y_{wdn} \times m_{wdn} \times c_{wdn} + Y_{fe} \times m_{fe} \times c_{fe} + Y_{st} \times m_{mp} \times c_{mp} + O_{oil} \times m_{oil} \times c_{oil} \tag{17}$$

where:

Y_{wdn}: ratio of the transformer winding losses to the total losses
Y_{fe}: ratio of the transformer core losses to the total losses
Y_{st}: ratio of the transformer stray losses to the total losses
m_{wdn}: weight of the transformer winding (kilograms)
m_{fe}: weight of the transformer core (kilograms)
m_{mp}: weight of the transformer tank and fittings (kilograms)
m_{oil}: weight of the transformer oil (kilograms)
c_{wdn}: transformer winding specific heat capacity ($c_{Cu} = 0.11 and c_{Al} = 0.25 Wh/kg^{\circ}C$)
c_{fe}: specific heat capacity of the transformer core ($c_{fe} = 0.13 Wh/kg^{\circ}C$)
c_{mp}: specific heat capacity of the transformer tank and fittings ($c_{mp} = 0.13 Wh/kg^{\circ}C$)
c_{oil}: specific heat capacity of the transformer oil ($c_{oil} = 0.51 Wh/kg^{\circ}C$)
O_{oil}: transformer oil correction factor for the ONAF and OFAF cooling types ($O_{oil} = 0.86 Wh/kg^{\circ}C$)

The oil thermal capacitance of the transformer without external cooling can be expressed as follows: [10]

$$C_{th-oil} = m_{wdn} \times c_{wdn} + m_{fe} \times c_{fe} + m_{mp} \times c_{mp} + m_{oil} \times c_{oil} \tag{18}$$

Eq. (15) is modelled to simulate TOT of the mineral oil and the alternative oils for the three scenarios of loading PF considering the impact of all thermal properties of them. Fig. 8, 9, 10 show TOT variation all day long for 0.85, 0.9, and 0.95 lagging PF respectively. At the instant of the curve peak, it is found TOT of mineral oil is the lowest one and that of Midel 1204 is the highest one of the different types of oils. For 0.85, 0.9, and 0.95 lagging PF, TOT of mineral oil is lower than that of Midel 7131 by 1.89 °C, 2.31 °C, and 2.61 °C respectively at the instant of the profiles peak. For the dedicated values of PF, TOT of mineral oil is less than that of Midel 1204 by 5.11 °C, 5.12 °C, and 5.08 °C respectively at the instant of the profiles peak.

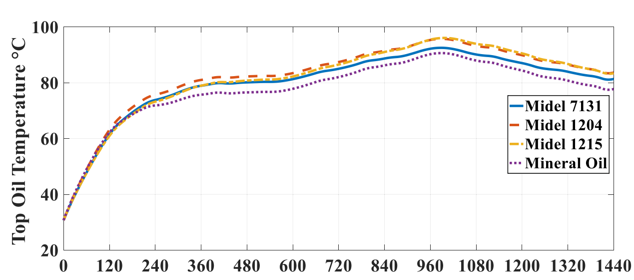

Fig. 8. TOT for mineral oil, Midel 7131, Midel 1204, and Midel 1215 at 0.85 lag PF.

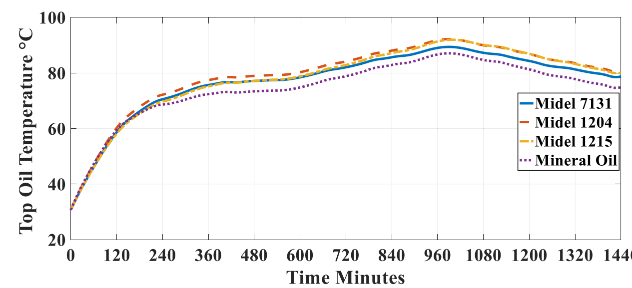

Fig. 9. TOT for mineral oil, Midel 7131 Midel 1204, and Midel 1215 at 0.9 lag PF.

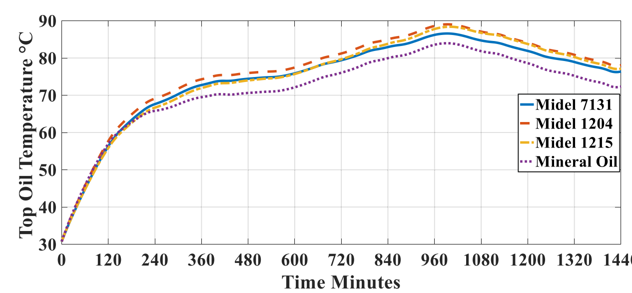

Fig. 10. TOT for mineral oil, Midel 7131, Midel 1204, and Midel 1215 at 0.95 lag PF.

5.2. Winding hot spot temperature model

The calculated TOT is used as input for the winding HST model. Hence, the thermal parameters of the different types of oil will affect the winding HST. The distribution of the winding temperature is not symmetrical. The winding HST is the hottest part of the winding which can deteriorate the transformer or decrease its normal life time. Hence, the winding HST shouldn't exceed the reference limit to keep the real life time as the normal expected life time. Fig. 11 shows the structure of building HST model into MATLAB [28]. The winding HST can be calculated as follows [27]:

$$K^2 \times \left(K_{\theta} + \frac{P_{EC-Rpu}}{K_{\theta}}\right) \times \mu_{pu}^{n''} \times \Delta\theta_{hs,rated} = \mu_{pu}^{n''} \times \tau_{wdg,rated} \times \frac{d\theta_{hs}}{dt} + \frac{(\theta_{hs} - \theta_{oil})^{1+n'}}{\Delta\theta_{hs,rated}^{n'}} \tag{19}$$

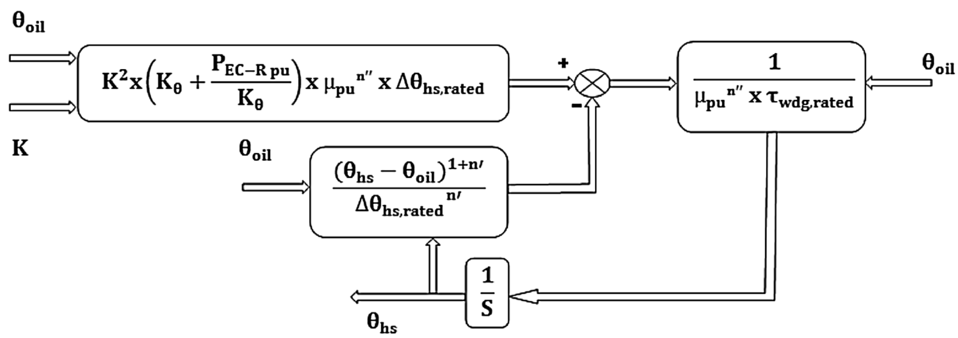

Fig. 11. Block diagram of the hot spot temperature model.

$$K_\theta = \frac{\theta_K + \theta_{hs}}{\theta_K + \theta_{avg}} \quad (20)$$

where:

θ_{hs}: operating winding HST (°C)
$\Delta\theta_{hs,rated}$: rated winding HST rise over TOT (°C)
P_{EC-Rpu}: pu unit eddy current losses at hot spot location under rated conditions
n': cooling constant for oil moving fluid
$\tau_{wdg,rated}$: time constant of winding at rated conditions (minutes)
K_θ: correction of the resistance on account of temperature change
θ_K: temperature factor for the loss correction
θ_{avg}: average temperature of the winding under rated conditions
$\theta_K = 225$: for Aluminum
$\theta_K = 235$: for Copper

Eq. (19) is modelled to simulate HST in cases of the mineral oil and the alternative oils for the three scenarios of loading PF considering the impact of all thermal properties of them. The losses of the transformer at different temperatures are obtained by considering the temperature-based correction of the resistance given in Eq. (20). Fig. 12, 13, 14 show HST variation all day long for 0.85, 0.9, and 0.95 lagging PF respectively. At the instant of the curve peak, it is found HST of mineral oil is the lowest one and that of Midel 1204 is the highest one of the different types of oils. For 0.85, 0.9, and 0.95 lagging PF, HST of mineral oil is lower than that of Midel 7131 by 3.6 °C, 4.3 °C, and 4.9 °C respectively at the instant of the profiles peak. For the dedicated values of PF, HST of mineral oil is less than that of Midel 1204 by 11.3 °C, 11.2 °C, and 11 °C respectively at the instant of the profiles peak. At the instant of the HST profile peak, the results show the transformer loadability filled with Midel 7131 is the highest one. In [29,30], HST reference for the mineral oil is 110 °C and for the ester is 131 °C.

6. Aging model

The reliability of the electrical network will be increased when the transformer real life time has been kept as expected normal life time.

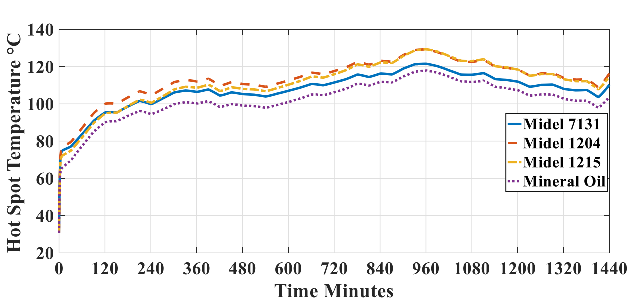

Fig. 12. HST for mineral oil, Midel 7131, Midel 1204, and Midel 1215 at 0.85 lag PF.

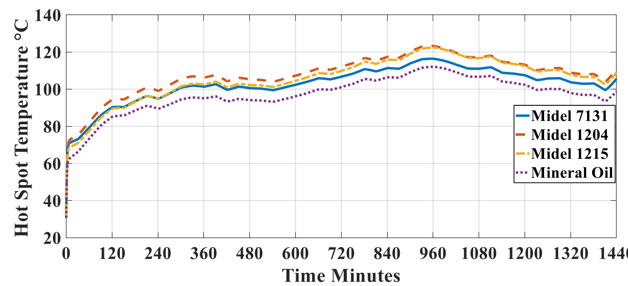

Fig. 13. HST for mineral oil, Midel 7131, Midel 1204, and Midel 1215 at 0.9 lag PF.

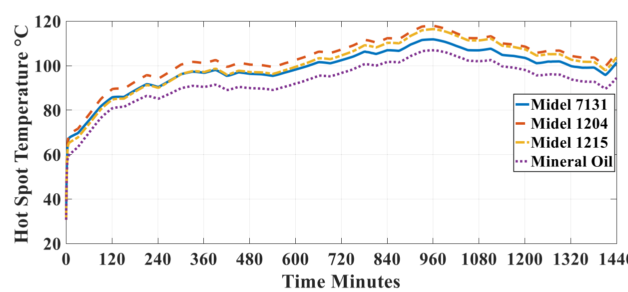

Fig. 14. HST for mineral oil, Midel 7131, Midel 1204, and Midel 1215 at 0.95 lag PF.

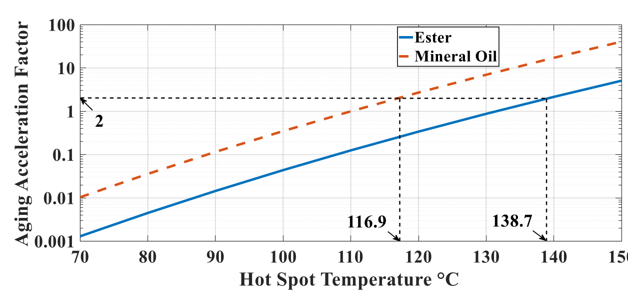

Fig. 15. Calculated aging acceleration factor versus the winding HST for mineral oil and ester.

Hence, it is mandatory to keep the transformer winding HST is less than the HST limit. A designation factor for the transformer aging is called aging acceleration factor (F_{AA}). It can be modelled as in Eq. (22). In case of mineral oil, it shows if the winding HST increased by 6.9 °C than the thermal limit of 110 °C, F_{AA} will be doubled and the real life time is half of the expected normal life time. But in case of esters, F_{AA} will be doubled if the winding HST increased by 7.7 °C than the thermal limit of 131 °C as shown in Fig. 15. The transformer loss of life (L_f) can be formulated during period of time dt as in Eq. (24). Fig. 16 shows that for the same winding HST of 110 °C, the ester-filled transformer have p.u life more than eight times that of mineral oil-filled transformer

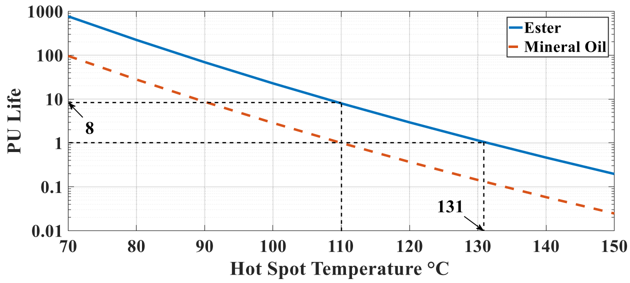

Fig. 16. Calculated pu life versus the winding HST for mineral oil [29] and ester [30].

[28,31].

$$\text{Per unit life} = A \ x \ e^{\left[\frac{15000}{\theta_H + 273}\right]} \tag{21}$$

$$F_{AA} = e^{\left[\frac{15000}{B} - \frac{15000}{\theta_H + 273}\right]} \tag{22}$$

$$dL = F_{AA} dt \tag{23}$$

$$L_f = \frac{1}{T} \int_0^T F_{AA} dt \tag{24}$$

where:

$A = 9.8 \times 10^{-18}$: for mineral oil
$A = 7.82 \times 10^{-17}$: for esters
$B = 383$: for mineral oil
$B = 404$: for esters

Eq. (24) is modelled to simulate the loss of life all day long of the mineral oil and the alternative oils for the different scenarios of the loading PF. Fig. 17, 18, 19 show the loss of life of the Midel 7131 is the lowest one and the mineral oil is the highest one as shown in Table 12. For Midel 7131, the results show the load power factor enhancement by 5% from 0.85 to 0.9 lagging PF led to enhancement of the transformer aging by 38.5%. But that for 10% from 0.85 to 0.95 lagging PF led to enhancement of the transformer aging by 60.6%. Also Midel 7131 succeeded in achieving the lowest aging for 0.85, 0.9 and 0.95 lagging PF. In case of 0.95 lagging PF, Midel 7131 reduced the aging by 76.67% than that of mineral oil. Hence, Midel 7131 is the best alternative to the mineral oil. Midel 1215 under 0.9 lagging load PF can be used as alternative to Midel 7131 under 0.85 lagging load PF for achieving the same or a little less aging. Table 12 can be used to find other alternatives to Midel 7131 and mineral oil for achieving the same or a little less aging but under different loading PF. Hence, not only the thermal properties of the cooling medium have a great impact on the transformer aging but also the loading power factor has.

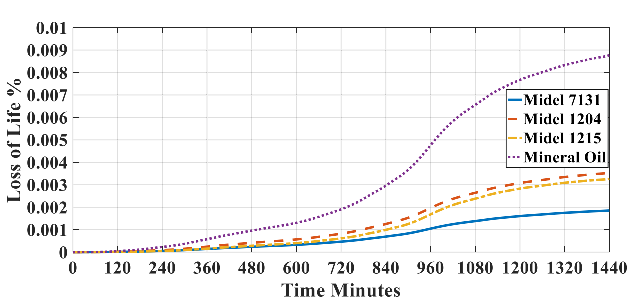

Fig. 17. Daily loss of life for mineral oil, Midel 7131, Midel 1204, and Midel 1215 at 0.85 lag PF.

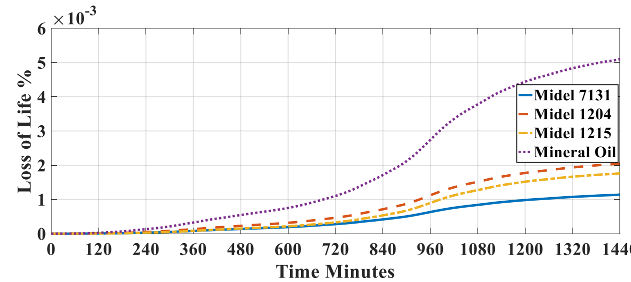

Fig. 18. Daily loss of life for mineral oil, Midel 7131, Midel 1204, and Midel 1215 at 0.9 lag PF.

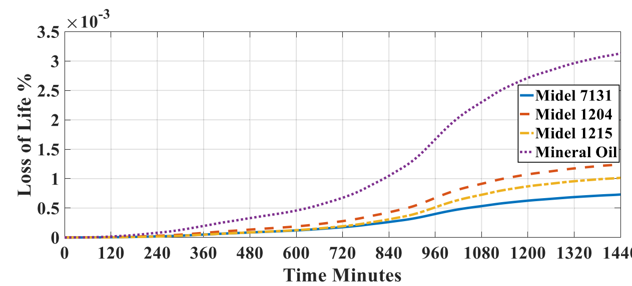

Fig. 19. Daily loss of life for mineral oil, Midel 7131, Midel 1204, and Midel 1215 at 0.95 lag PF.

Table 12
The annual percent loss of life for mineral oil, Midel 7131, Midel 1204, and Midel 1215 at different load PF,

Load lagging PF	0.85	0.9	0.95
Mineral Oil (LOL%)	3.2	1.8615	1.1432
Midel 7131 (LOL%)	0.6774	0.4165	0.2667
Midel 1204 (LOL%)	1.2903	0.7479	0.4544
Midel 1215 (LOL%)	1.1903	0.6431	0.3701

7. Cost effectiveness and environmental assesment

For making decisions to select one solution instead of another one based on the economic aspects, the engineering economy should be applied. The engineers should evaluate the expected consequence of the profitability analysis. They use mathematical formulation to investigate and analyze the alternatives of engineering design and select the best solution [32]. The investment into the electrical energy is rapidly increasing, so the cost of the electrical energy losses should be reduced for more profit. Transformers with more cost effectiveness are necessary to be used for the electrical utility and the transformer users [33]. In this paper, we investigate the perturbation and improved load PF on the cost effectiveness of the transformer filled with the mineral, Midel 7131, Midel 1204, and Midel 1215 oil. The transformer bid price is constant for the different cases of load PF and oil types. But, the cost of

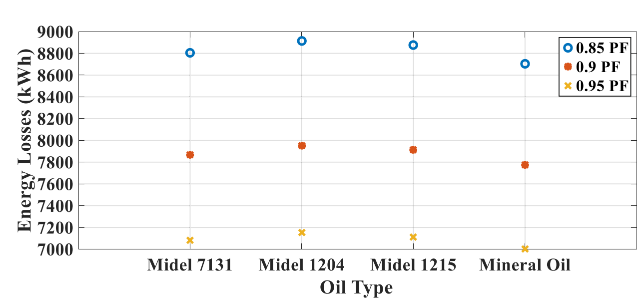

Fig. 20. Monthly transformer energy losses for the different scenarios of load PF and considering the different types of oils.

transformer energy losses relies on the load PF, the transformer oil thermal parameters, and the ambient temperature. The ambient temperature is considered all day long. The monthly energy losses of the transformer for the different scenarios of load PF and considering the different types of oils are shown in Fig. 20. Fig. 20 shows the monthly energy losses of mineral oil achieve the minimum values but that of Midel 1204 are the maximum for the three scenarios of the loading PF. The cost of the transformer total energy losses are as follows:

$$C_{TL} = DPY \times ET \int_0^T (NLL + LL \times K^2)dt \quad (25)$$

$$LL = PxK_\theta + \frac{P_{EC-R}}{K_\theta} + P_{OSL} \quad (26)$$

where:

C_{TL}: cost of the transformer energy losses (LE/year)
NLL: no-load losses (kW)
LL: load losses under rated conditions (kW)
P: ohmic losses (kW)
P_{EC-R}: rated eddy current losses (kW)
P_{OSL}: other stray losses in the structural parts (kW)
DPY: day per year
ET: electricity tariff (1.05 LE/kWh)

If the transformer energy losses are reduced, the emissions of the green houses gases (GHG) because of combustion of fossil fuel for generation plants will be decreased. GHG emissions will cost the government to raise the health care. Hence, this cost is defined as an environmental cost. If the load PF can be controlled, the environmental cost can be minimized.

For the preservation of the environment, many countries put GHG emissions limit. If the energy users or utilities transcend this limit, they have to pay penalty or buy credits of GHG from other that have excess of GHG credits. Hence, the environmental cost should be involved in the investigation of the transformer cost effectiveness. To investigate the environmental cost because of the transformer total energy losses, the existing year cost factor (LE/MWh) of the GHG emissions should be calculated as follows: [34]

$$C = C_y \sum_{j=1}^{N} f_j \times e_j \quad (27)$$

$$e_j = \left(e_{CO_2,j} + 21e_{CH_4,j} + 310e_{N_2O,j}\right)\frac{0.0036}{n_j(1-\lambda_j)} \quad (28)$$

where:

C_y: the charge of the existing year GHG emissions (900LE/t_{co_2})
t_{co_2}: equivalent tonnes of carbon dioxide emissions
j: fuel type
N: fuels counter of energy mixture
f_j: the percentage of the consuming energy coming from fuel type j
e_j: the emission factor of fuel type j (t_{co_2}/MWh)
$e_{CO_2,j}$: the emission factor of carbon dioxide for fuel type j (kg/GJ)
$e_{CH_4,j}$: the emission factor of methane for fuel type j (kg/GJ)
$e_{N_2O,j}$: the emission factor of nitrous oxide for fuel type j (kg/GJ)
λ_j: the percentage of energy losses in the utility for fuel type j
n_j: the conversion efficiency for fuel type j (%)

The environmental parameters in [35] are considered to evaluate the perturbations and improved load PF impacts on the environmental cost. Methane, carbon dioxide, and nitrous oxide are the considered GHG emissions. The GHG emissions due to combustion of fossil fuel are shown in Table 13. For evaluating the GHG emissions on account of the transformer total energy losses, the emission factors are multiplied by the total energy losses of the transformer.

Table 13
Contributions of fossil fuel plants in GHG emissions.

Fuel type	Natural gas	Diesel	Coal
f_j%	15	7.6	69.77
$e_{CO_2,j}$ kg/GJ	56.1	74.1	94.6
$e_{CH_4,j}$ kg/GJ	0.003	0.002	0.002
$e_{N_2O,j}$ kg/GJ	0.001	0.002	0.003
λ_j%	8	8	8
n_j%	45	30	35

Table 14
Annual Transformer Energy Losses, its Cost, and its Impact on the Environmental Cost.

Load PF	0.85	0.9	0.95
Mineral Oil			
Annual Transformer Energy Losses (kWh)	105,898.67	94,583.67	85,166.67
C_{TL}(LE/year)	111,193.6	99,312.85	89,425
EC(LE/year)	85,129.8	76,033.9	68,463.8
SEC(LE/year)	–	9,095.9	16,666
t_{co_2}	94.6	84.5	76.1
Midel 7131			
Annual Transformer Energy Losses (kWh)	107,103.17	95,703	86,188.67
C_{TL}(LE/year)	112,458.33	100,488.15	90,498.1
EC(LE/year)	86,098.1	76,933.7	69,285.3
SEC(LE/year)	–	9,164.4	16,812.8
t_{co_2}	95.7	85.5	77
Midel 1204			
Annual Transformer Energy Losses (kWh)	108,441.5	96,749.33	87,028.17
C_{TL}(LE/year)	113,863.58	101,586.8	91,379.58
EC(LE/year)	87,174	77,774.9	69,960.2
SEC(LE/year)	–	9399.1	17,213
t_{co_2}	96.9	86.4	77.7
Midel 1215			
Annual Transformer Energy Losses (kWh)	108,003.5	96,274.83	86,541.5
C_{TL} (LE/year)	113,403.68	101,088.57	90,868.58
EC (LE/year)	86,821.9	77,393.4	69,569
SEC (LE/year)	–	9,428.5	17,252.9
t_{co_2}	96.5	86	77.3

The environmental cost and the saving into the environmental cost due to the difference of the improved PF than 0.85 lagging PF are formulated as follows:

$$EC = DPY \times C \times 10^{-3} \times \int_0^T (NLL + LL \times K^2)dt \quad (29)$$

$$SEC = DPY \times C \times LL \times 10^{-3} x \int_0^T (\Delta K^2)dt \quad (30)$$

where:

EC: the existing year environmental cost (LE/year)
SEC: the saving into the existing year environmental cost (LE/year)
ΔK^2: the difference between the square of loading

Table 14 shows the annual transformer energy losses, the annual transformer energy losses cost, the environmental cost, and the equivalent tonnes of carbon dioxide emissions of mineral oil are the lowest one but that of Midel 1204 are the highest one. For Midel 7131, the annual transformer energy losses, the annual transformer energy losses cost, the environmental cost, and the equivalent tonnes of carbon dioxide emissions under 0.95 lagging PF are lower than that under 0.85

lagging PF by 19.5%. But for the same previous quantities under 0.9 lagging PF are lower than that under 0.85 lagging PF by 10.2%.

8. Conclusion

This paper evaluated the impact of using environmentally friendly oils on the winding hottest spot temperature, the transformer aging, the transformer energy losses cost, and the environmental cost in comparison to mineral oil. Synthetic ester (Midel 7131), rapeseed (Midel 1204), and soya (Midel 1215) were used as environmentally friendly oils that are commercially produced. To calculate the rated TOT and HST, the models of the thermal properties were built into COMSOL. Then, TOT and HST were obtained all day long under wide range of the operating temperatures through using thermal equivalent circuit into MATLAB. For ester oils, the thermal parameters were evaluated experimentally on a wide temperature range from −10 °C to 100 °C. The experimental results were fit to find out a best representative formula suitable for implementation into the model. The simulation results show that the thermal parameters of the mineral oil caused lower top oil and winding hottest spot temperatures than that of Midel 7131, Midel 1204, or Midel 1215. But, from the aging point of view, ester oils succeeded in achieving the lowest aging at various values of loading PF. This was attributed to no free water and significantly less paper degradation for ester case. Midel 7131 exhibited the best aging performance, where it could reduce the transformer aging by 76.67% at 0.95 lagging PF and 78.8% at 0.85 lagging PF than that of the mineral oil. But, Midel 1215 reduced the transformer aging by about 67.6% at 0.95 lagging PF and 62.8% at 0.85 lagging PF than that of the mineral oil. Midel 7131 in case of 0.95 lagging PF succeeded in achieving 19.5% reduction for the annual energy losses, annual transformer energy losses cost, environmental cost, and equivalent tonnes of carbon dioxide emissions than that in case of 0.85 lagging PF. But for 0.9 lagging PF, the reduction is 10.2% than that in case of 0.85 lagging PF. Hence, the thermal parameters of the oil to fill the transformer and the transformer loading power factor should be considered in the planning stage. The planner can use Midel 7131 under 0.85 lagging PF as an alternative to the mineral oil under 0.95 lagging PF. This concept can increase the safety, add more environmental benefits, reduce the aging of the transformer by 40.75%, and avoid the needed cost for enhancing the loading PF by 10%.

References

[1] Georgilakis PS. Spotlight on Modern Transformer Design. Springer-Verlag London; 2009.
[2] Susa D, Lehtonen M, Nordman H. Dynamic thermal modeling of distribution transformers. IEEE Trans Power Delivery 2005;20(3):1919–29.
[3] Nadolny Z, Dombek G, Przybylek P. Thermal properties of a mixture of mineral oil and synthetic ester in terms of its application in the transformer. 2016 IEEE Conference on Electrical Insulation and Dielectric Phenomena (CEIDP). 2016. p. 857–60.
[4] Mehta DM, Kundu P, Chowdhury A, Lakhiani VK, Jhala AS. A review on critical evaluation of natural ester vis-à-vis mineral oil insulating liquid for use in transformers: Part I. IEEE Trans Dielect Elect Insul 2016;23(2):873–80.
[5] Mehta Dhruvesh M, Kundu P, Chowdhury A, Lakhiani VK, Jhala AS. A review on critical evaluation of natural Ester vis-à-vis mineral oil insulating liquid for use in transformers: part II. IEEE Trans Dielect Elect Insul 2016;23(3):1705–12.
[6] Rafiq M, Lv YZ, Zhou Y, Ma KB, Wang W, Li CR, et al. Use of vegetable oils as transformer oils – a review. Renew Sustain Energy Rev 2015;52:308–24.
[7] Sankaran C. Power Quality. CRC Press; 2002.
[8] Dugan RC, McGranaghan MF, Santoso S, Beaty HW. Electrical Power Systems Quality. 2nd ed. McGraw-Hill; 2003.
[9] Zobaa AF, Bansal R, Manana M. Power Quality Monitoring, Analysis and Enhancement. IntechOpen 2011.
[10] Susa D, Lehtonen M. Dynamic thermal modeling of power transformers: further development—part I. IEEE Trans Power Delivery 2006;21(4):1961–70.
[11] Susa D, Nordman H. A simple model for calculating transformer hot-spot temperature. IEEE Trans Power Delivery 2009;24(3):1257–65.
[12] Asano R, Page SA. Reducing environmental impact and improving safety and performance of power transformers with natural ester dielectric insulating fluids. IEEE Trans Ind Appl 2014;50(1):134–41.
[13] Xu Y, Qian S, Liu Q, Wang ZD. Oxidation stability assessment of a vegetable transformer oil under thermal aging. IEEE Trans Dielect Elect Insul 2014;21(2):683–93.
[14] Lecuna R, Delgado F, Ortiz A, Castro PB, Fernandez I, Renedo CJ. Thermal-fluid characterization of alternative liquids of power transformers: a numerical approach. IEEE Trans Dielect Elect Insul 2015;22(5):2522–9.
[15] Bandara K, Ekanayake C, Saha TK, Annamalai PK. Understanding the ageing aspects of natural ester based insulation liquid in power transformer. IEEE Trans Dielect Elect Insul 2016;23(1):246–57.
[16] Mansour DA, Ammar AM. Performance evaluation of environmentally friendly insulating oil under accelerated aging tests. Eighteenth International Middle East Power Systems Conference (MEPCON), Cairo; 2016. pp. 927–931.
[17] Zhang X, Daghrah M, Wang Z, Liu Q, Jarman P, Negro M. Experimental verification of dimensional analysis results on flow distribution and pressure drop for disc type windings in OD cooling modes. IEEE Trans Power Delivery 2017;33(4):1647–56.
[18] Santisteban A, Delgado F, Ortiz A, Fernández I, Renedo CJ, Ortiz F. Numerical analysis of the hot-spot temperature of a power transformer with alternative dielectric liquids. IEEE Trans Dielect Elect Insul 2017;24(5):3226–35.
[19] Hoffmann J-F, Vaitilingomb G, Henry J-F, Chirtoc M, Olives R, Goetz V, et al. Temperature dependence of thermophysical and rheological properties of seven vegetable oils in view of their use as heat transfer fluids in concentrated solar plants. Solar Energy Mater Solar Cells 2018;178:129–38.
[20] Zhang X, Wang Z, Liu Q, Jarman P, Negro M. Numerical investigation of oil flow and temperature distributions for ON transformer windings. Appl Therm Eng 2018;130:1–9.
[21] Bergman TL, Lavine AS, Incropera FP, DeWitt DP. Fundamentals of Heat and Mass Transfer. Seventh Edition John Wiley & Sons Inc; 2011.
[22] Cengel Y, Ghajar A. Heat and Mass Transfer: Fundamentals and Applications. Fifth Edition McGraw-Hill Education; 2015.
[23] Bouhaddiche R, Bouazabia S, Fofana I. Thermal modelling of power transformer. 19th IEEE International Conference on Dielectric Liquids (ICDL), Manchester, United Kingdom, 25–29 June. 2017.
[24] Daghrah M, Wang Z, Liu Q, Hilker A, Gyore A. Experimental study of the influence of different liquids on the transformer cooling performance. IEEE Trans Power Delivery 2019;34(2):588–95.
[25] Abbas A, Abou Elzahab E, Elbendary A. Thermal modeling and ageing of transformer under harmonic currents. 23rd International Conference on Electricity Distribution, Lyon, 15-18 June. 2015.
[26] Salama MMM, Mansour DA, Abdelmaksoud SM, Abbas AA. Impact of long-term climatic conditions on the ageing and cost effectiveness of the oil-filled transformer. Twentieth International Middle East Power Systems Conference (MEPCON), Cairo University, Egypt, 18-20 Dec. 2018. p. 494–9.
[27] Cui Y, Ma H, Saha T, Ekanayake C, Martin D. Moisture-dependent thermal modelling of power transformer. IEEE Trans Power Deliv 2016;31(5):2140–50.
[28] Paterakis NG, Pappi IN, Erdinç O, Godina R, Rodrigues EMG, Catalão JPS. Consideration of the impacts of a smart neighborhood load on transformer aging. IEEE Trans Smart Grid 2016;7(6):2793–802.
[29] IEEE Guide for Loading Mineral-Oil-Immersed Transformers, IEEE Standard C57.91-1995; 1996.
[30] Luksich J. Loading Guide A and B Factors for Envirotemp FR3 Fluid and Thermally Upgraded Kraft Insulation. Eng. Dev. Report TP03-DR-009, Cooper Power Systems; 2003.
[31] Kweon D, Koo K, Woo J, Kim Y. Hot spot temperature for 154 kV transformer filled with mineral oil and natural ester fluid. IEEE Trans Dielect Elect Insul 2012;19(3):1013–20.
[32] Leland Blank, Anthony Tarquin, Engineering Economy, eighth edition, New York, USA; 2018.
[33] Charalambous CA, Milidonis A, Lazari A, Nikolaidis AI. Loss evaluation and total ownership cost of power transformers—Part I: a comprehensive method. IEEE Trans Power Deliv 2013;28(3):1872–80.
[34] Georgilakis PS, Amoiralis EI. Distribution transformer cost evaluation methodology incorporating environmental cost. IET Gener Transm Distrib 2010;4(7):861–72.
[35] Salama MMM, Mansour DA, Abdelmakasoud SM, Abbas AA. Impact of optimum power factor of PV controlled inverter on the aging and cost effectiveness of oil-filled transformer considering long-term characteristics. IET Gener Transm Distrib. 2019;13(16):3574–82.